AGU PUBLICATIONS

JGR

Journal of Geophysical Research: Atmospheres

RESEARCH ARTICLE
10.1002/2014JD022044

Special Section:
Fast Physics in Climate Models: Parameterization, Evaluation and Observation

Aerosol transport over the western Mediterranean basin: Evidence of the contribution of fine particles to desert dust plumes over Alborán Island

A. Valenzuela[1,2], F. J. Olmo[1,2], H. Lyamani[1,2], M. J. Granados-Muñoz[1,2], M. Antón[3], J. L. Guerrero-Rascado[1,2], A. Quirantes[1], C. Toledano[4], D. Perez-Ramírez[5,6], and L. Alados-Arboledas[1,2]

[1]Departamento de Física Aplicada, Universidad de Granada, Granada, Spain, [2]Grupo de Física de la Atmósfera, IISTA, Universidad de Granada, Granada, Spain, [3]Departamento de Física, Universidad de Extremadura, Badajoz, Spain, [4]Grupo de Óptica Atmosférica, Universidad de Valladolid, Valladolid, Spain, [5]Mesoscale Atmospheric Processes Laboratory, NASA Goddard Space Flight Center, Greenbelt, Maryland, USA, [6]Goddard Earth Sciences Technology and Research, University Space Research Association (GESTAR/USRA), Columbia, Maryland, USA

Key Points:
- Optical properties in the almucantar and principal plane configurations
- Anthropogenic particles were transported together desert dust from North Africa
- Low values of single scattering albedo during desert dust events

Correspondence to:
A. Valenzuela,
avalenzuela@ugr.es

Citation:
Valenzuela, A., F. J. Olmo, H. Lyamani, M. J. Granados-Muñoz, M. Antón, J. L. Guerrero-Rascado, A. Quirantes, C. Toledano, D. Perez-Ramírez, and L. Alados-Arboledas (2014), Aerosol transport over the western Mediterranean basin: Evidence of the contribution of fine particles to desert dust plumes over Alborán Island, *J. Geophys. Res. Atmos.*, *119*, doi:10.1002/2014JD022044.

Received 16 MAY 2014
Accepted 3 DEC 2014
Accepted article online 8 DEC 2014

Abstract Eight months (June 2011 to January 2012) of aerosol property data were obtained at the remote site of Alborán Island (35.95°N, 3.03°W) in the western Mediterranean basin. The aim of this work is to assess the aerosol properties according to air mass origin and transport over this remote station with a special focus on air mass transport from North Africa. For air masses coming from North Africa, different aerosol properties showed strong contributions from mineral dust lifted from desert areas. Nevertheless, during these desert dust intrusions, some atmospheric aerosol properties are clearly different from pure mineral dust particles. Thus, Angström exponent α(440–870) presents larger values than those reported for pure desert dust measured close to dust source regions. These results combine with $\alpha(440, 670) - \alpha(670, 870) \geq 0.1$ and low single scattering albedo ($\omega(\lambda)$) values, especially at the largest wavelengths. Most of the desert dust intrusions over Alborán can be described as a mixture of dust and anthropogenic particles. The analyses support that our results apply to North Africa desert dust air masses transported from different source areas. Therefore, our results indicate a significant contribution of fine absorbing particles during desert dust intrusions over Alborán arriving from different source regions. The aerosol optical depth data retrieved from Sun photometer measurements have been used to check Moderate Resolution Imaging Spectroradiometer retrievals, and they show reasonable agreement, especially for North African air masses.

1. Introduction

During recent decades, an enormous effort has been made to determine the effects of atmospheric aerosols on climate. However, due to their large spatiotemporal variability and the variety of aerosol mixtures, there are still significant uncertainties about understanding aerosol optical and microphysical properties, which result in uncertainties about the effects of atmospheric aerosols on climate via radiative forcing [*Intergovernmental Panel on Climate Change*, 2013].

The Mediterranean Basin is of special interest for the study of atmospheric aerosols due to its strategic geographic location surrounded by continents with different surface characteristics. Due to its geography, local winds, complex coastlines, and orography have strong influences on the Mediterranean atmospheric flow. For this reason, numerous studies have been conducted over its Western area [e.g., *Smirnov et al.,* 1995; *Silva et al.,* 2002 and *Pereira et al.,* 2011; *Lyamani et al.,* 2006a; *Toledano et al.,* 2007; *Estellés et al.,* 2007; *Cachorro et al.,* 2008; *Prats et al.,* 2008; *Valenzuela et al.,* 2012a, 2014], in the central Mediterranean [e.g., *Pace et al.,* 2006; *Tafuro et al.,* 2006; *Meloni et al.,* 2006, 2008; *Di Biagio et al.,* 2009; *Perrone and Bergamo*, 2011], and in the Eastern Mediterranean [e.g., *Smirnov et al.,* 1995; *Gerasopoulos et al.,* 2003, 2006, 2009; *Kaskaoutis et al.,* 2011]. The western Mediterranean basin receives different aerosol types, including desert dust from arid zones of the African continent, anthropogenic aerosols from industrialized areas in Europe, and marine aerosols from the North Atlantic Ocean and the Mediterranean Sea [e.g., *Lyamani et al.,* 2006a; *Pace et al.,* 2006; *Gerasopoulos et al.,* 2009]. The seasonal distribution of the different atmospheric aerosol types in the Mediterranean Basin is controlled by local, regional, synoptic, and large-scale circulation [e.g., *di Sarra et al.,* 2001]. Furthermore, anthropogenic particles emitted from the intense ship traffic in the Mediterranean Sea represent an additional source [e.g., *Viana et al.,* 2009; *Pandolfi et al.,* 2011; *Becagli et al.,* 2012]. Ship emissions

have become an important source of air pollution in the Mediterranean Basin, and it is foreseen that in the future, this pollution source will even exceed other aerosol sources over land [*Cofala et al.,* 2007].

Aerosol properties clearly depend on the aerosol origin. Thus, when air masses are transported from North African to the Mediterranean Basin, high aerosol optical depths and low Angström exponents are often observed [e.g., *Pace et al.,* 2006]. The cleanest atmospheric conditions in the Mediterranean Basin, which are characterized by low aerosol optical depth, are usually found when air masses are advected from the North Atlantic Ocean [e.g., *Pace et al.,* 2006; *Toledano et al.,* 2007; *Gerasopoulos et al.,* 2009; *Toledano et al.,* 2009]. In this sense, *Lyamani et al.* [2014] found that clean maritime conditions were observed over Alborán Island on 40% of the analyzed days with aerosol optical depth (AOD) (500 nm) < 0.15 and α is lower than 1 for North Atlantic Ocean air masses.

Aerosol optical properties at their origin, as issued by the sources, are influenced by potential changes during transport as well as by the local aerosol properties at the reception site [e.g., *Hand et al.,* 2010; *Bauer et al.,* 2011]. Thus, it is highly interesting to study the transport of atmospheric aerosols from North Africa to Europe to understand their potential mixing with anthropogenic fine aerosols and to quantify changes in reference to their desert origin.

Backward trajectory analysis is a well-known technique to link air mass origin (and/or pathway) with aerosol optical properties at the receptor site [e.g., *Pace et al.,* 2006; *Estellés et al.,* 2007; *Xia et al.,* 2007; *Toledano et al.,* 2009; *Kaskaoutis et al.,* 2011; *Rozwadowska et al.,* 2010; *Gerasopoulos et al.,* 2011; *Valenzuela et al.,* 2012a]. The analysis of backward trajectories provides objective interpretations related to the source regions, residence times over each region and different circulation patterns (curvature and length) of air masses. Even taking into account that the accuracy of backward trajectories shows position errors of up to 20% of the travel distance [*Stohl*, 1998], trajectories are a useful tool to study the circulation patterns of air masses.

Aerosol characterization on small islands is of great interest because it can provide information on aerosol properties over relatively large scale transport [e.g., *Di Biagio et al.,* 2009]. In this sense, several authors have monitored aerosol optical and microphysical properties in remote places [e.g., *Dubovik et al.,* 2002 and *Toledano et al.,* 2011; *Pace et al.,* 2006 and *Meloni et al.,* 2006]. Many efforts are being made to characterize aerosol types and aerosol long-range transport over sea and ocean remote areas from ground-based measurements, leading to the setup of the Maritime Aerosol Network (MAN) as part of the Aerosol Robotic Network (AERONET) network [*Smirnov et al.,* 2009]. However, the absence of continuous measurements provided by the MAN network can be replaced by measurements on remote islands, which can act as permanent platforms to characterize aerosol properties that are generally unaffected by local anthropogenic sources. Additionally, ground-based stations on these islands, where the albedo of the surrounding surface is homogeneous, can provide appropriate platforms to validate satellite measurements, helping to improve the accuracy of satellite retrieval techniques at regional scales. Alborán Island, located between the North African coast and the Southern Iberian Peninsula, offers an appropriate location to perform studies focused on the characterization of aerosol optical and microphysical properties advected from different areas (Europe, Africa, and North Atlantic Ocean) or for the validation of satellite data.

The main objective of this work is to analyze the columnar aerosol optical and microphysical properties over Alborán Island (35.95°N, 3.03°W) according to the air masses affecting the region. Using data gathered from June 2011 to January 2012, we put special emphasis on air masses coming from North Africa to assess the contribution of anthropogenic fine particles during desert dust events. In addition, due to its reduced dimensions and the homogeneous albedo of the surrounding surface, we compare the aerosol properties obtained by Sun photometer over Alborán Island with Moderate Resolution Imaging Spectroradiometer (MODIS) data. It is worth noting that in this work we use sky radiance measurements in the principal plane configuration, which enlarge the data set of atmospheric aerosol properties in combination with the analysis of measurements in the almucantar plane.

2. Experimental Site and Instrumentation

The remote Alborán Island (35.95°N, 3.01°W, 15 m above sea level) is located 90 km from the Southern Iberian Peninsula and 50 km from the Northern African coast (Figures 1a and 1b). In this region, summers are usually

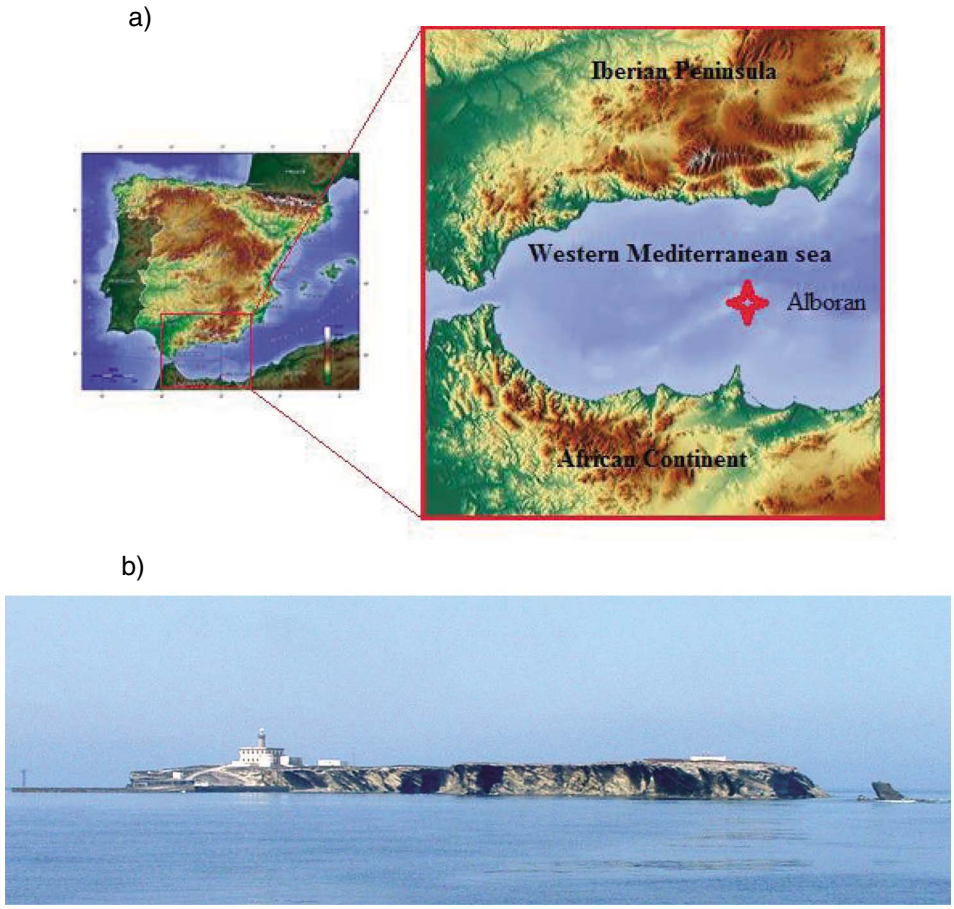

Figure 1. (a) Geographic location and (b) image of Alborán Island.

dry and hot due to the influence of the atmospheric subtropical high-pressure belt [e.g., *Sumner et al.,* 2001]. During winter, the subtropical high shifts south, allowing midlatitude storms to enter the region from the Atlantic, and bringing enhanced amounts of rainfall to the Mediterranean. Anomalous torrential rainfalls occur during this season in response to severe storms that are generated locally by extreme atmospheric convective overturn [e.g., *Romero et al.,* 1999]. Alborán is an uninhabited island without local sources of anthropogenic aerosol, such that background conditions are driven by the marine aerosol contribution; however, the island is just south of an important shipping route that could contribute to anthropogenic fine particles over the island. Due to its small size, with an area of 0.072 km^2, and to its strategic location, Alborán Island constitutes an ideal station to characterize aerosol optical and microphysical properties advected from different areas (Europe, Africa, and North Atlantic Ocean).

The measurements were recorded by a Cimel Sun photometer (Cimel CE-318-4) operated as part of the AERONET network [*Holben et al.,* 1998] on the roof of a military complex on Alborán Island from June 2011 to January 2012. This instrument has eight channels covering the spectral range 340–1020 nm for direct Sun measurements and four channels (440, 670, 870, and 1020 nm) for sky radiances collected in the almucantar and principal plane configurations. Direct Sun measurements are performed every 15 min, while sky radiances measurements depend on an optical air mass protocol.

The Sun photometer was calibrated by the AERONET-EUROPE team (http://aeronet.gsfc.nasa.gov), and a linear rate change was assumed for the calibration coefficients. To enlarge the data set of atmospheric aerosol properties, we have applied our own procedures to retrieve aerosol optical depth (AOD) and aerosol microphysical properties (from the inversion of both almucantar and principal plane radiance measurements), which are summarized in section 3 and explained in more detail by *Valenzuela et al.* [2012c].

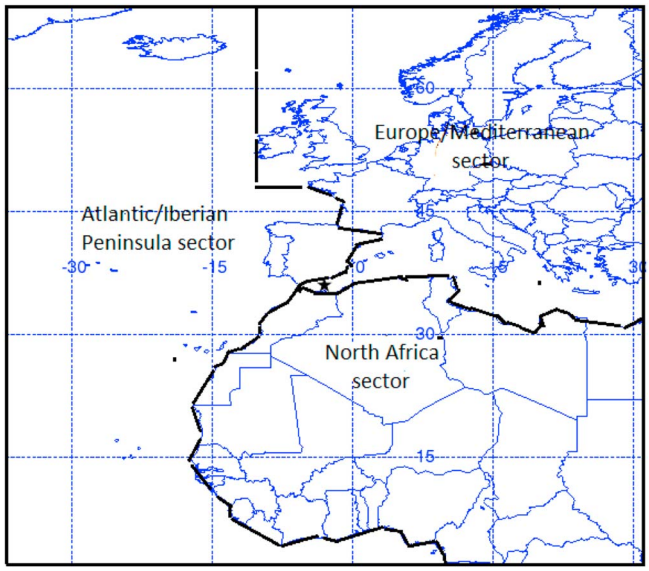

Figure 2. Different source regions are split into three sectors (European/Mediterranean, North African, and Atlantic/Iberian Peninsula sectors).

3. Methodology

3.1. Sun Photometer

Direct Sun measurements are used to retrieve the spectral aerosol optical depth at the eight spectral channels from 340 to 1200 nm and the Angström exponent (440–870 nm). The methodology was described in detail by *Alados-Arboledas et al.* [2003, 2008]. The total ozone column over the study site was provided by the Ozone Monitoring Instrument on board the AURA satellite (http://aura.gsfc.nasa.gov/instruments/omi.html).

The applied inversion algorithm uses the almucantar and principal plane sky radiances measured by the Cimel instrument [*Olmo et al.,* 2006, 2008; *Valenzuela et al.,* 2012c]. The original Nakajima inversion method [*Nakajima et al.,* 1996] has been adapted to consider nonspherical particles. Taking into account this procedure, a wide set of optical and microphysical aerosol parameters were derived, such as the columnar aerosol size distribution, single scattering albedo, and asymmetry parameter. A detailed description of this inversion method (a cloud screening algorithm, accuracy of individual retrievals, and a sensibility test) can be found in *Valenzuela et al.* [2012b, 2012c].

3.2. Air Masses Classification Over Alborán Island

In this work, a set of air mass back trajectories arriving at Alborán Island has been generated using a HYSPLIT_4.9 model including vertical winds [*Draxler and Rolph*, 2003]. We used 5 day backward trajectories with endpoints at 12:00 UTC over Alborán Island at three different levels, 500, 1500 and 3000 m above ground level, using the Global Data Analysis System meteorological data. To associate the aerosol radiative properties with specific regional influences, we have classified the air mass backward trajectories, taking into account potential aerosol origin sources. To identify possible aerosol source sectors, we assume that the aerosol particles are confined into the boundary layer at the source region and that the air mass is laden with aerosol particles when its altitude (h) is lower or closer to the altitude of the boundary layer (h'). The geographical sector where this condition is fulfilled along the trajectory is identified as the source of the detected aerosol. If the entrainment condition is fulfilled at more than one point, the geographical position selected as the potential source of aerosol particles is that in which the absolute difference between h and h' is the lowest. Three regions, the Central Europe-Mediterranean Sea sector, the North African sector, and the Atlantic Ocean and Iberian Peninsula sector, have been identified as potential source regions of aerosols, as displayed in Figure 2. This method has been broadly used to identify aerosol sources (e.g., *Pace et al.* [2006], *Petzold et al.* [2008] in Morocco, and *Valenzuela et al.* [2012b]). During the study period, the most frequent air masses affecting Alborán Island originated on the Atlantic/Iberian Peninsula (48% of the cases) and from North African sectors (31% of the cases). Most of the African desert dust intrusions over Alborán Island were favored by a high pressure (observed from sea level to 700 hPa) centered north of Argelia, with an associated high pressure over the western African continent. In contrast, Atlantic/Iberian Peninsula air masses over Alborán Island were favored in most cases by two synoptic situations, a low pressure over the Iberian Peninsula associated with high pressure (observed from sea level to 700 hPa) centered over the Atlantic Ocean and an anticyclone over the North Atlantic Ocean associated with high pressure over the Mediterranean Sea. The most frequent meteorological scenario related to the air masses transport from the European/Mediterranean sector was a low pressure centered over northwestern Africa and a high pressure (observed from sea level to 850 hPa) centered over central Europe (figure not shown).

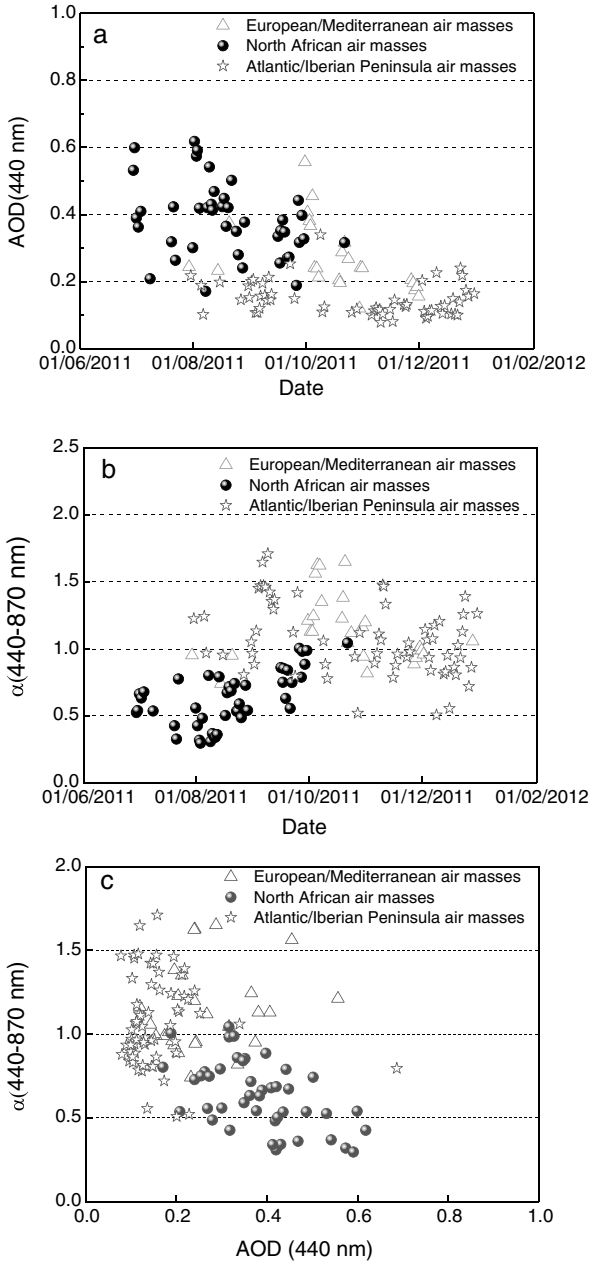

Figure 3. Temporal evolution of daily mean: (a) AOD (440 nm) and (b) α(440–870 nm) values over Alborán Island according to the aerosol origin classification. (c) Correlation between AOD (440 nm) and α(440–870 nm) for each origin sector.

3.3. MODIS

The Moderate Resolution Imaging Spectroradiometer (MODIS) on board the Terra and Aqua satellites is part of NASA's Earth Observing System (EOS) mission. The Terra satellite (EOS AM-1) crosses the equator daily at 10:30 A.M., moving south (descending mode), while Aqua (EOS PM-1) crosses the equator daily at 01:30 P.M. LT (local time) as it moves north (ascending mode). The MODIS sensor provides aerosol properties on a daily basis every 1–2 days, with a repetition cycle of 16 days. The sensor has 36 spectral channels from visible to infrared wavelengths (410 to 15,000 nm). Data are acquired with three spatial resolutions (250, 500, and 1000 m pixel size at the nadir), depending on the spectral band [e.g., *Ichoku et al.,* 2004]. Two different algorithms (one over land and one over ocean) are applied due to the different surface properties [e.g., *Remer et al.,* 2005; *Kaufman et al*., 1997; *Tanré et al.,* 1997; *Levy et al.,* 2005].

MODIS/Aqua and MODIS/Terra level 2 data (Collection 0051) are used in this study. MODIS level 2 data provide global AOD over land and ocean at a spatial resolution of 10 × 10 km. AOD at 550 nm over ocean data are used in this work. The prelaunch uncertainty (theoretical error) of the MODIS AOD is ±0.03 ± 0.05 (AOD) over the ocean [e.g., *Chu et al.,* 1998, 2002; *King et al.,* 1999; *Remer et al.,* 2002].

4. Results and Discussion

4.1. Aerosol Optical and Microphysical Properties According to Source Regions

A total of 5996 cloud-free measurements (158 days) were performed from June 2011 to January 2012. Figures 3a and 3b show the temporal evolution of the daily mean values of AOD (440 nm) and the Angström exponent, α(440–870 nm), taking into account the aerosol source sectors. High AOD associated with low α values (e.g., 30 June and 1–3 and 9 August) were found when air masses were transported from the North African sector, indicating large contributions of coarse particles to aerosol loading. From summer (July/August) to autumn (September/October), the AOD values decreased while α increased for the North African sector. A lower predominance of coarse particles (desert dust contributions) is evident for several days in September and October. During the whole period, the mean AOD (440 nm) for the North African sector was 0.38 ± 0.13, which is comparable to that found by *Pace et al.* [2006] and *Meloni et al.* [2007] during desert dust events over Lampedusa Island (Table 1). The mean AOD value for the North African sector was also close to that reported by *Toledano et al.* [2009] in "El Arenosillo," African dust episodes that occurred in southwestern Spain from 2000 to 2004 (Table 1).

Table 1. Comparison of Aerosol Optical Properties With Those Obtained in Other Locations

Authors	Air Masses Origin	AOD(±SD)	α(±SD)	Location
Pace et al. [2006]	North Africa	0.36 ± 0.16 at 495.7 nm	0.4 ± 0.4 at 415.6–868.7 nm	Lampedusa Island, Italy
Pace et al. [2006]	Central-Eastern Europe	0.23 ± 0.11 at 495.7 nm	1.5 ± 0.4 at 415.6–868.7 nm	Lampedusa Island, Italy
Meloni et al. [2007]	North Africa	0.35 ± 0.01 at 500 nm	0.30 ± 0.02 at 415.5–868.5 nm	Lampedusa Island,Italy
Toledano et al. [2009]	North Africa	0.35 ± 0.19 at 440 nm	0.6 ± 0.4 at 440–870 nm	El Arenosillo, Spain
This study	North Africa	0.38 ± 0.13 at 440 nm	0.6 ± 0.2 at 440–870 nm	Alborán Island, Spain
This study	European/Mediterranean	0.27 ± 0.12 at 440 nm	1.2 ± 0. 3 at 440–870 nm	Alborán Island, Spain
This study	Atlantic/Iberian Peninsula	0.15 ± 0.08 at 440 nm	1.1 ± 0. 4 at 440–870 nm	Alborán Island, Spain

At Alborán Island, the mean α(440–870 nm) value for the North African sector was 0.6 ± 0.2, comparable to that of 0.6 ± 0.4 found by *Toledano et al.* [2009] during Saharan dust events over southwestern Spain. The mean α(440–870 nm) value retrieved in our study during desert dust intrusions was slightly higher than the reported value for pure dust aerosols (approximately 0.3 or lower) near dust source regions [*Tesche et al.,* 2009]. However, the mean α(440–870 nm) value obtained here was similar to that obtained in Ras El Ain during the SAMUM experiment (mean α(440–870 nm) value of 0.58) for a mixture of dust and fine particles [*Toledano et al.,* 2009]. This suggests a mixing of desert dust with fine particles or a reduction in the mean particle size during dust transport to Alborán, which is likely associated with the deposition of the largest dust particles. Furthermore, we analyze key aerosol parameters, such as fine-mode fraction and single scattering albedo, to evaluate whether desert dust observed over Alborán was mixed with fine particles from other origins.

In contrast to air masses from the North African sector, air masses transported from the Atlantic/Iberian Peninsula sector showed low mean AOD (440 nm) (0.15 ± 0.08) and relatively high mean α(440–870 nm) (1.1 ± 0.4) values. The α(440–870 nm) values obtained for this sector ranged from 0 to 2, indicating different atmospheric situations dominated by different aerosol types (coarse particles, fine aerosols, and different mixtures of both coarse and fine particles). The Atlantic air masses passed over the Iberian Peninsula before reaching Alborán, and thus, emissions from urban-industrial areas in the Iberian Peninsula could contribute to the observed large variability in α(440–870 nm) for this sector. Furthermore, part of this variability may be attributed to the large uncertainty in the α(440–870 nm) parameter for low AOD [e.g., *Holben et al.,* 1998; *Wagner and Silva*, 2008].

A mean AOD (440 nm) value of 0.27 ± 0.12 associated with a relatively large mean α(440–870 nm) value of 1.2 ± 0.3 was observed when air masses were transported from the European/Mediterranean sector. The transport of the air masses from this sector occurred mainly in autumn (Figure 3a). The AOD (440 nm) and α(440–870 nm) values obtained in this sector indicate a predominance of fine-mode aerosol particles during aerosol transport from this sector.

Due to its location, marine aerosol is expected to be one of the major components of background conditions on Alborán Island. However, on some days, maritime aerosol over Alborán can be masked by aerosols transported from the European and African continents, although it is present in the boundary layer during the entire measurement period. According to *Smirnov et al.* [2002], "pure maritime" aerosol conditions are characterized by low aerosol loads and Angström exponents (AOD $<$ 0.15 and α(440–870) $<$ 1). In this sense, pure maritime situations associated with AOD $<$ 0.15 and α(440–870) $<$ 1 were found only in the Atlantic/Iberian Peninsula category (Figure 3). We found that only 33% of the data included in the Atlantic/Iberian Peninsula category (40% of all data) were associated with pure maritime situations.

The scatterplot of α(440–870 nm) versus AOD is a useful tool to identify different aerosol types. Whereas AOD mainly depends on the aerosol load, α(440–870 nm) is related to the size of the predominant aerosol [e.g., *Kaufman et al.,* 1998; *Eck et al.,* 1999; *Smirnov et al.,* 2000; *Dubovik et al.,* 2002; *Pace et al.,* 2006; *Toledano et al.,* 2007; *Prats et al.,* 2008]. Figure 3c shows three main clusters of particles corresponding to the three aerosol source regions considered. There were clear differences between the aerosol properties of the atmospheric aerosols transported by the different air masses considered in our classification scheme (Figure 3c). As seen in Figure 3c, a large amount of data in the Atlantic/Iberian Peninsula category showed AOD values below 0.2, with α(440–870 nm) values ranging from 0.5 to 1.7, indicating different atmospheric background conditions dominated by different aerosol types (coarse particles, fine aerosols, and different mixtures of both coarse and fine particles). On the other hand, some cases with AOD higher than 0.3 (5%) were also observed when air mass was transported from the Atlantic/Iberian Peninsula sector. These cases are probably associated with drastic

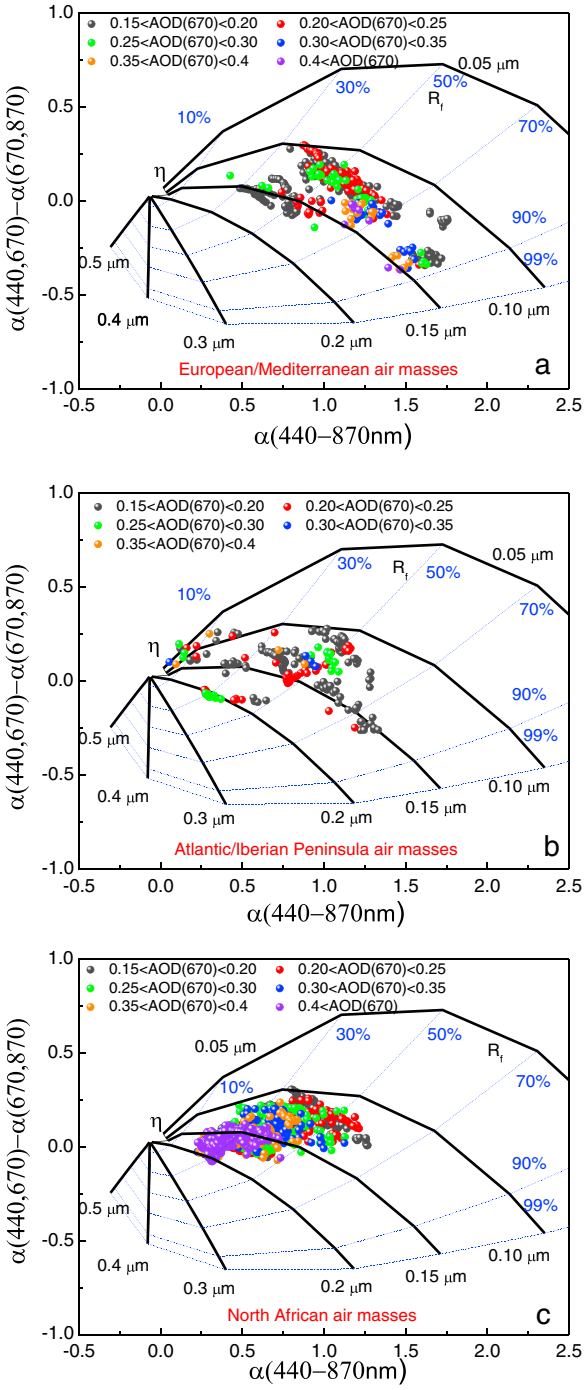

Figure 4. Angström exponent difference, $\delta\alpha = \alpha(440, 670) - \alpha(670, 870)$, as a function of α(440–670) and AOD (670 nm) for (a) European/Mediterranean sector, (b) Atlantic/Iberian Peninsula sector, and (c) North African sector . Solid lines represent the fine-mode radius, and dashed line represents the contribution percentage of fine-mode fraction to the aerosol optical depth.

change in air masses on these days or with the significant contribution of emissions from urban-industrial areas or occasional forest fires on the Iberian Peninsula. Air masses from the North African sector exhibited a predominance of high AOD linked to low α(440–870 nm), indicating large contributions of coarse particles during transport from the African continent. It is worth mentioning that a small amount of data included in the North African category showed α(440–870 nm) values close to 1 or slightly larger than 1, suggesting a relevant contribution of fine particles during these cases. The European/Mediterranean sector yielded AOD values in the range 0.2–0.6 with α(440–870 nm) mainly above 1, typical of fine-mode aerosol from urban/industrial activities [*Dubovik et al.,* 2002].

In view of the results obtained in this first analysis, the aerosol optical properties observed over Alborán depended on the air mass types affecting the site study. Therefore, a detailed analysis of optical properties based on air mass origin is presented in the following paragraphs.

The fine-mode fraction of AOD (η) is a useful parameter for distinguishing aerosol types and mixtures from Sun photometer measurements. Thus, to discriminate different aerosol types using η parameter, we used the simple graphical method proposed by *Gobbi et al.* [2007]. This technique has been proven to be very robust for tracking and characterizing mixtures of pollution aerosol and mineral dust [*Gobbi et al.,* 2007; *Basart et al.,* 2009]. This method gives a first approximation of the fine-mode fraction (η) and fine modal radius (R_f) and thus allows us to quantify the contribution of fine-mode particles to AOD using a single approach that does not require complex microphysical retrieval. Furthermore, this technique allows us to separate AOD increases due to the increase in coarse particle contribution from AOD increases due to fine particle growth by coagulation and/or humidification [*Gobbi et al.,* 2007; *Basart et al.,* 2009]. We have used the AOD (670 nm) to classify aerosol properties as a function of α(440–870 nm) and its spectral curvature, represented by $\delta\alpha = \alpha(440, 670) - \alpha(670, 870)$. The Angström parameter usually remained below 1. *Kaufman* [1993] established that strong negative values ranging from −0.5 to −0.3 indicate the dominance of aerosol fine mode. *Basart et al.* [2009] found that when dominated by coarse aerosol particles, such as desert dust,

Table 2. Spectral Single Scattering Albedo at 440 and 1020 nm Wavelengths for Each Aerosol Origin Sector

Authors	Air Masses Origin	ω(440 nm) (±SD)	ω(1020 nm) (±SD)	Location
Dubovik et al. [2002]	Desert dust	0.93 ± 0.01	0.99 ± 0.01	Cape Verde
Dubovik et al. [2002]	Urban-industrial and mixed	0.90 ± 0.02	0.83 ± 0.02	Mexico City, Mexico
Dubovik et al. [2002]	Urban-industrial and mixed	0.94 ± 0.03	0.91 ± 0.03	Paris, France
Dubovik et al. [2002]	Urban-industrial and mixed	0.91 ± 0.03	0.84 ± 0.03	Maldives
Lyamani et al. [2006a, 2006b]	Dust and anthropogenic aerosol mixed	0.89 ± 0.02	0.88 ± 0.02	Granada, Spain
Lyamani et al. [2006a, 2006b]	European/Mediterranean	0.92 ± 0.02	0.84 ± 0.02	Granada, Spain
Valenzuela et al. [2012b]	Dust and anthropogenic aerosol mixed	0.89 ± 0.03	0.91 ± 0.03	Granada, Spain
This study	Desert dust	0.88 ± 0.03	0.91 ± 0.03	Alborán Island, Spain
This study	European/Mediterranean	0.86 ± 0.03	0.84 ± 0.05	Alborán Island, Spain
This study	Atlantic/Iberian Peninsula	0.88 ± 0.03	0.85 ± 0.05	Alborán Island, Spain

$\delta\alpha$ tends to be negative or slightly positive, with values in the range of -0.3 to 0.1. Values of $\delta\alpha$ larger than 0.1 indicate the contribution of fine-mode fractions and coarse-mode fractions in the calculation of AOD. Gobbi's diagrams, classified by sectors, are shown in Figure 4. For this computation, we have only employed values of AOD (670 nm) > 0.15 to avoid errors in α(440–870 nm) larger than 30% [*Gobbi et al.,* 2007]. Air masses from the Atlantic/Iberian Peninsula sector showed a large number of observations with AOD (670 nm) lower than this threshold, which were not included in Gobbi's diagram.

For the European/Mediterranean sector (Figure 4a), the increase in AOD is linked to a shift to larger α(440–870 nm) values with more negative $\delta\alpha$, indicating an increase in the fine-mode contribution for larger AODs. In this sense, there was a small group of data in the upper range of α(440–870 nm) and the lowest range of $\delta\alpha$ ($1.3 \le \alpha(440\text{–}870\,\text{nm}) \le 1.7$ and $-0.1 \le \delta\alpha \le -0.3$) presenting large extinction (AOD >0.3), which corresponds to $0.80\% \le \eta \le 90\%$ and $r_f \sim$ (0.10–0.13 μm). Thus, these cases were associated with a strong contribution of fine particles with rather small fine-mode radius, which could be related to the influence of anthropogenic fine particles emitted in polluted European areas and the Mediterranean Sea [e.g., *Pace et al.,* 2006].

Figure 4b shows that different aerosol types (size and aerosol load) were associated with the Atlantic/Iberian Peninsula sector because $\delta\alpha$ ranged from -0.25 to 0.3, indicating that some cases were dominated by large particles, likely sea salt, others by fine anthropogenic particles originating from the Iberian Peninsula and the rest by a mixture of these two aerosol types. The group of observations with α(440–870 nm) values ranging from 0.25 to 0.75, which corresponds to $\eta \le 40\%$ and $0.15 \le r_f \le 0.20$ μm, could be related to coarse particles, likely sea salt originating from the Mediterranean Sea.

The North African sector (Figure 4c) accounted for up to 95% of the observations with $\eta < 50\%$ and $\alpha < 1$ with $\delta\alpha$ between -0.16 and 0.25. For this category, the increase in AOD was associated with a shift of α(440–870 nm) to lower values, with $\delta\alpha$ close to zero, indicating an increasing contribution of coarse particles to the total AOD. *Basart et al.* [2009] showed that "pure mineral" dust particles present $\delta\alpha \le 0$, α(440–870 nm) < 0.3, and $\eta < 40\%$. In our case, only a few data points associated with AOD >0.35 corresponded to pure mineral dust particles. However, there were significant cases with $\delta\alpha \ge 0.1$, α(440–870 nm) < 1 and $\eta < 50\%$, which were associated with the mixture of coarse mineral dust with fine-mode particles [*Basart et al.,* 2009]. The small group of observations with $\eta > 50\%$ and $0 \le \delta\alpha$ could be explained by the significant contribution of fine particles to total AOD in these dusty cases. These fine particles were possibly associated with anthropogenic particles originating in urban-industrial areas in North Africa that were advected with desert dust particles [e.g., *Rodríguez et al.,* 2011] or with anthropogenic fine particles from ship emissions and/or from polluted European regions. Finally, in the North African sector, unlike the other two sectors, we observed that the fine particles mode experienced growth processes as indicated by the increase in the radius of the fine mode

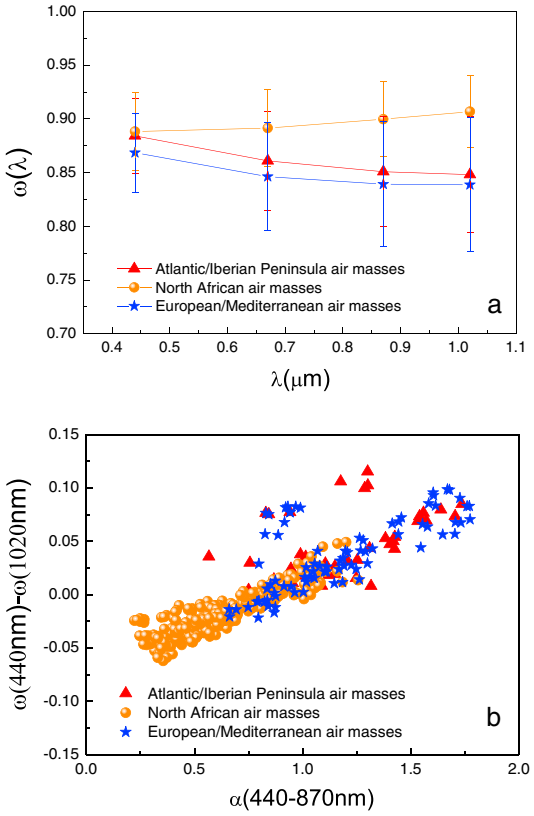

Figure 5. (a) Single scattering albedo for European/Mediterranean, North African, and Atlantic/Iberian Peninsula sectors and (b) difference of ω(440 nm) − ω(1020 nm) versus Angström exponent for three aerosol origin sources.

withincreasing AOD, as seen in Figure 4c. In fact, for $0.2 < \text{AOD} < 0.25$, the fine-mode radius was found to be approximately 0.12 μm, while for $\text{AOD} > 0.4$, the fine-mode radius increased up to 0.2 μm.

Table 2 presents the average values and corresponding standard deviations of $\omega(\lambda)$ at the 440 and 1020 nm wavelengths obtained for the three aerosol origin sources over the entire measurement period. The retrieved $\omega(\lambda)$ for each aerosol sector origin showed large variability, as indicated by the associated standard deviations (Table 2). This large $\omega(\lambda)$ variability could be related, in part, to the different mixtures of different aerosol types and to the degree to which each aerosol component contributed to the aerosol load in each sector category, depending on the residence time and the altitude of the transported air mass over the source sector. It is worth noting that the ω(440 nm) values were almost similar for the three aerosol sector sources (Table 2). The small differences in ω(440 nm) among the various aerosol categories associated with the different source regions can represent the advantage in satellite retrievals of AOD at shorter wavelengths of the visible range, because single scattering albedo must be assumed a priori in many satellite retrieval algorithms [e.g., *Eck et al.,* 2010]. The spectral dependence of $\omega(\lambda)$ obtained for both the European/Mediterranean and the Atlantic/Iberian Peninsula sectors was significantly different to that obtained for the North African sector (Figure 5a). As seen in Figure 5a, $\omega(\lambda)$ decreased with increasing wavelength for the European/Mediterranean and the Atlantic/Iberian Peninsula sectors, which is an indication of less scattering at longer wavelengths related to a reduction in the contribution of coarse particles for these sectors. This spectral dependence of $\omega(\lambda)$ is a feature of anthropogenic and biomass burning particles [e.g., *Dubovik et al.,* 2002; *Lyamani et al.,* 2006a, 2006b]. The mean $\omega(\lambda)$ values obtained for the European/Mediterranean sector were slightly lower than those obtained for the Atlantic/Iberian Peninsula sector, indicating a slightly larger contribution of absorbing particles (i.e., black carbon) during the air mass transport from the European/Mediterranean sector than from the Atlantic/Iberian Peninsula sector. The retrieved $\omega(\lambda)$ for the European/Mediterranean and Atlantic/Iberian Peninsula sectors were lower, especially for shorter wavelengths, than the values reported by *Dubovik et al.* [2002] for urban-industrial aerosols in Paris, Mexico City, and Maldives and were also lower than those obtained by *Lyamani et al.* [2006a, 2006b] in Granada, Spain, under anthropogenic pollution conditions during the severe 2003 summer heat wave (Table 2). These results suggest that the aerosol mixtures over Alborán during the air mass transport from the European/Mediterranean and the Atlantic/Iberian Peninsula sectors contained a significant fraction of fine absorbing aerosol types (i.e., black carbon).

As expected, $\omega(\lambda)$ increased slightly with wavelength for the North African sector, which is a typical characteristic of desert dust [e.g., *Dubovik et al.,* 2002; *Lyamani et al.,* 2006a, 2006b; *Valenzuela et al.,* 2012b]. However, $\omega(\lambda)$ values obtained for the North African sector were lower, especially in the largest wavelengths, than those reported for pure desert dust measured close to dust source regions and were similar to those reported for dust mixed with anthropogenic particles (Table 2). In addition, $\omega(\lambda)$ values retrieved during desert dust intrusions over Alborán (a site with no local anthropogenic sources) were similar or slightly lower than those found by *Lyamani et al.* [2006a, 2006b] and *Valenzuela et al.* [2012b] during desert dust events over Granada (a site with significant local anthropogenic sources). This result suggests a significant contribution of anthropogenic absorbing fine particles to the total aerosol load during African dust intrusions

over Alborán. The low $\omega(\lambda)$ values obtained for the North African sector were probably caused by the lifting of fine anthropogenic absorbing particles (i.e., black carbon) during dust transport over North African urban/industrial areas [*Rodríguez et al.,* 2011] and/or to the coexistence over Alborán of desert dust and fine absorbing particles emitted from ships or transported from urban-industrial European areas.

Derimian et al. [2008] used the difference between ω(440 nm) and ω(1020 nm) to discriminate aerosol types in terms of aerosol absorption properties. This approach presents two advantages. First, it is expected that the difference will provide better accuracy than absolute values, because the retrieval of spectral dependence of $\omega(\lambda)$ is more reliable than that of an absolute value of $\omega(\lambda)$. Second, the spectral behavior of $\omega(\lambda)$ can be characterized by only one parameter, $d\omega = \omega(440\text{ nm}) - \omega(1020\text{ nm})$. Negative values of $d\omega$ are related to greater scattering by coarse particles at 1020 nm and to less contribution by anthropogenic fine particles, while positive values are related to the reduced scattering contribution of coarse particles and to stronger absorption at 1020 nm by black carbon particles. Values of $d\omega$ close to zero associated with Angström exponent values in the range 0.5–1.0 are related to mixtures of coarse particles and pollution [*Derimian et al.,* 2008]. Figure 5b shows $\omega(440\text{ nm}) - \omega(1020\text{ nm})$ versus α(440–870 nm) for the three aerosol categories considered in this study. This figure reveals that, in general, as α(440–870 nm) increased from approximately 0.2 to approximately 1.8, the difference $\omega(440\text{ nm}) - \omega(1020\text{ nm})$ became positive and larger, indicating a decreasing contribution of coarse dust particles and an increasing fraction of fine absorbing particles for the three sectors. A significant amount of data corresponding to both the European/Mediterranean and Atlantic/Iberian Peninsula sectors presented $d\omega > 0$ and $\alpha(440\text{–}870\text{ nm}) > 1$, indicating the significant contributions of fine absorbing particles (i.e., black carbon) and the reduced contributions of coarse particles (dust or sea salt) in these cases. However, there was a small amount of data in the European/Mediterranean and Atlantic/Iberian Peninsula sectors (2% and 9%, respectively) with $d\omega > 0$ and $\alpha(440\text{–}870\text{ nm}) < 0.8$, indicating mixed aerosol types in these cases. Given the relatively low $\alpha(440\text{–}870\text{ nm}) < 0.8$ and $d\omega > 0$, these small amounts of data may corresponded to a mixed aerosol type (coarse and fine particles) containing a significant proportion of nonabsorbing coarse particles (sea salt) and fine particles with considerable fractions of anthropogenic absorbing particles (i.e., black carbon). On the other hand, there was also a small amount of data in the European/Mediterranean sector (16%) with $0.8 < \alpha(440\text{–}870\text{ nm}) < 1.3$ and $d\omega$ close to zero, which correspond to aerosol mixtures (with different degrees of mixing) containing nonabsorbing coarse particles (sea salt) and fine particles with small fractions of fine absorbing particles.

In contrast, the North African sector showed small number of data points (5%) with $\alpha(440\text{–}870\text{ nm}) < 0.3$ and $d\omega < -0.025$, which correspond to "pure" desert dust. However, a significant number of data points (60%) in this sector presented $d\omega$ values close to zero and α(440–870 nm) values in the range 0.5–1.0, which were related to mixtures of coarse dust particles and fine pollution particles [*Derimian et al.,* 2008]. Furthermore, the North African sector also showed some data (25%) with $d\omega > 0$ associated with α(440–870 nm) values in the range 0.8–1.2. These cases were related to aerosol mixtures (dust and fine particles) with significant contributions of fine absorbing particles. These fine particles might have mixed with dust during desert dust transport over urban-industrial North African areas, an explanation that has been suggested in previous studies [e.g., *Rodríguez et al.,* 2011]. However, the contribution of North African fine particle during dust events over Alborán can be masked by anthropogenic fine particles accumulated over the Mediterranean Sea, especially during summer when desert dust events and stagnation conditions are more frequent. The mountainous terrain of the Iberian Peninsula to the north and the African continent to the south favor the occurrence of stagnation conditions and the accumulation of anthropogenic fine particles in the western Mediterranean region, as observed by *Millán et al.* [1996]. To investigate the possible role of the North African fine particles during dust events observed over Alborán, in section 4.2, we analyze the dependence of aerosol optical properties during these events on the different African dust source regions and dust transport pathways.

4.2. Aerosol Optical Properties According to the Different Desert Dust Transport Scenarios

In our previous analysis, we showed that during North African desert dust events, the aerosol optical properties retrieved over Alborán Island indicated that mineral particles were mixed with anthropogenic fine aerosol. According to *Rodríguez et al.* [2011], air masses from the North African sector could transport, depending on their transport pathways, anthropogenic particles emitted in North African urban-industrial

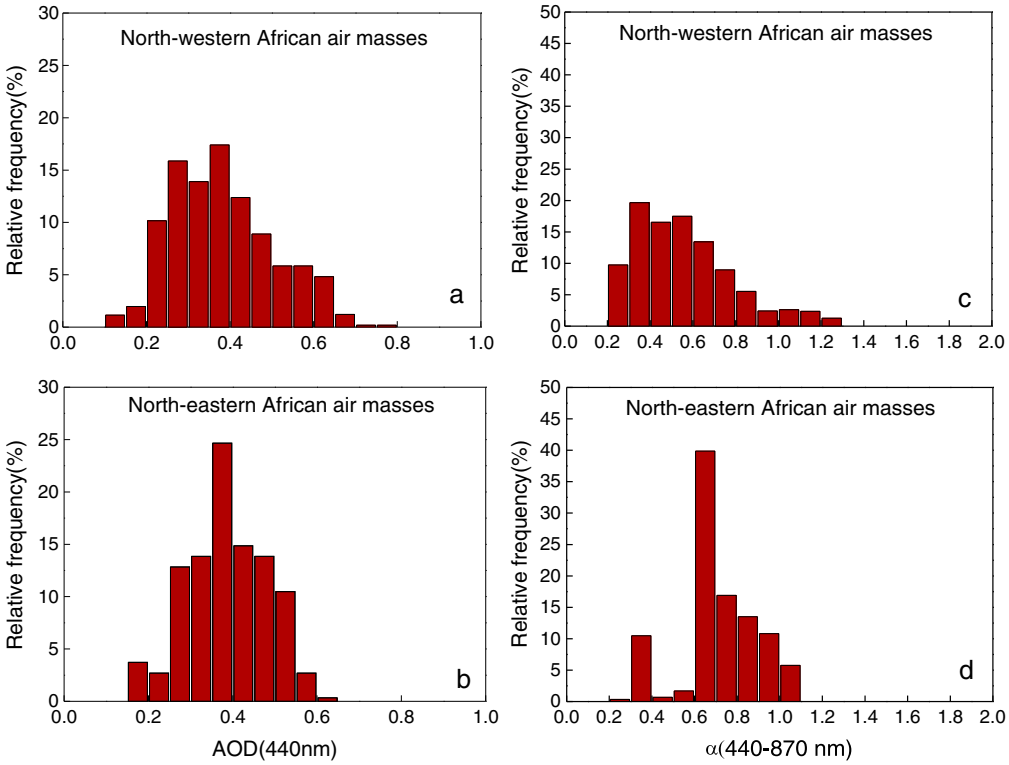

Figure 6. Frequency histograms of AOD at (a and b) 440 nm and (c and d) α(440–870 nm) for Northwestern (Figures 6a and 6c) and Northeastern (Figures 6b and 6d) air masses transported from North Africa.

areas together with the desert dust. To assess the possible role of these anthropogenic particles, we classified the air masses transported from North Africa according to their origin and pathways. In this sense, we have identified two main desert dust transport scenarios over Alborán: air masses which originated in northwestern Africa and passed through the coast of the Atlantic Ocean (78% of the cases) and air masses which originated in eastern Africa and traveled over the Mediterranean Sea (22% of the cases). It is interesting to note that whereas air masses from northwestern Africa passed over several urban industrial areas along the coast of Morocco, air masses originating in northeastern Africa reached Alborán Island without traversing too many anthropogenic aerosol sources. A total of 1753 and 335 Sun photometer measurements were performed in the northwestern African/Atlantic Ocean and the northeastern African/Mediterranean Sea transport, respectively.

Frequency histogram plots for the AOD (440 nm) and α(440–870 nm) for the two desert dust scenarios are shown in Figure 6. For the northwestern African/Atlantic Ocean scenario, the frequency histogram for AOD (440 nm) (Figure 6a) showed a main peak at 0.39, with 84% of observations included in the range from 0.23 to 0.53. The frequency histogram of α(440–870 nm) (Figure 6c) presented one mode centered at ~0.5, suggesting the predominance of coarse particles. However, up to 54% of the observations α(440–870 nm) showed values higher than 0.5, corresponding to the mixtures of dust with fine particles. For the northeastern African/Mediterranean Sea scenario (Figure 6b), AOD presented a monomodal distribution centered at 0.38, with 97% of the observations above 0.23. The frequency histogram of α(440–870 nm) (Figure 6d) showed an absolute maximum centered at 0.6, with 70% of the observations in the narrow range from 0.65 to 0.85, suggesting a relevant contribution of fine particles during these dusty cases [e.g., *Derimian et al.,* 2008]. These results revealed that AOD and α(440–870) obtained at Alboran Island did not show significant differences during the two main desert dust scenarios.

Figures 7a and 7b shows $\omega(\lambda)$ versus wavelength for α(440–870 nm) < 0.7 (situations dominated by coarse aerosol) and for α(440–870 nm)$>$0.7 (cases with a significant fine particle contribution) for North African transport scenarios. For α(440–870 nm) < 0.7 cases, $\omega(\lambda)$ increased slightly with wavelengths for both

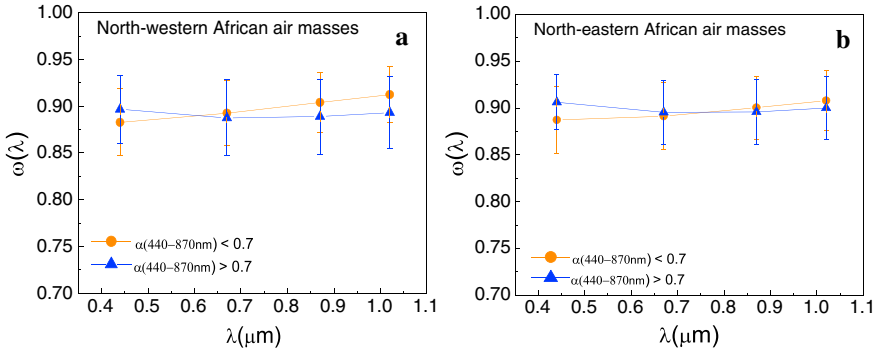

Figure 7. Single scattering albedo versus wavelength for (a) Northwestern Africa air masses and (b) Northeastern Africa air masses.

scenarios, which is a typical desert dust behavior. However, the increase of $\omega(\lambda)$ with wavelength was weaker, and $\omega(\lambda)$ values obtained in both transport scenarios were lower than the values typically observed for desert dust derived from Sun photometer measurements [e.g., *Dubovik et al.,* 2002b], indicating the significant absorbing aerosol contribution during both transport scenarios for α(440–870 nm) < 0.7 cases. For α(440–870 nm)$>$0.7 cases, $\omega(\lambda)$ also decreased with wavelength during both transport scenarios, suggesting again the relevant contribution of anthropogenic absorbing aerosols, such as black carbon [e.g., *Dubovik et al.,* 2002]. In general, we observed that $\omega(\lambda)$ values obtained during both transport scenarios were very similar for both α(440–870 nm) < 0.7 cases and α(440–870 nm)$>$0.7 cases.

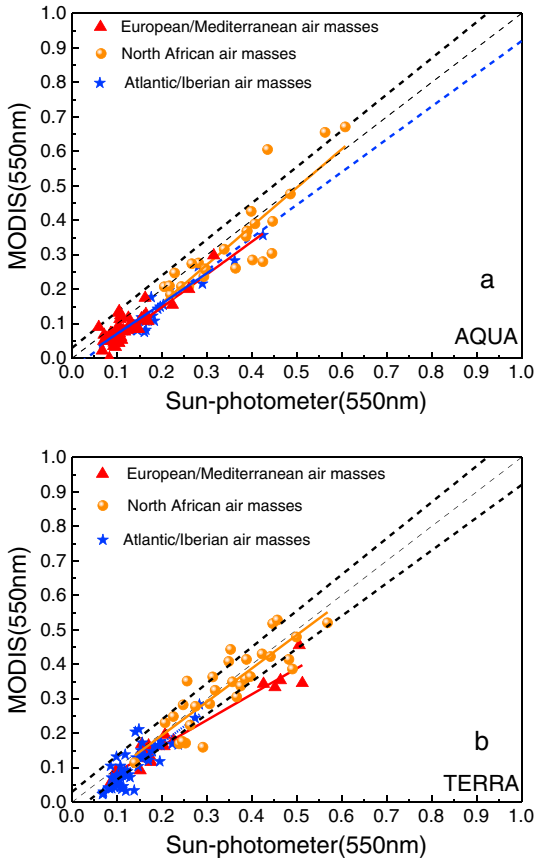

Figure 8. Scatterplot of the MODIS-retrieved AOD at 550 nm versus the AOD at 550 nm obtained from the Sun photometer for (a) Terra and (b) Aqua for each sector origin.

Therefore, as presented here, the aerosol properties (namely AOD, α(440–870), and $\omega(\lambda)$) did not show any significant changes depending on the origin and transport pathway of the air masses. According to these results, the influence of anthropogenic fine particles originating from the urban-industrial areas in the north of Africa during desert dust outbreaks can be assumed to be negligible, and the presence of the anthropogenic fine mode observed in our data can be attributed to a significant contribution of fine particles from urban-industrial European areas and/or ship emissions in the Mediterranean region.

4.3. MODIS Validation

Satellite measurements, such as those from MODIS, provide estimates of AOD that are relevant for regional studies; therefore, they could be very valuable in our study around Alborán Island due to its strategic location. A previous validation of MODIS AOD with our Sun photometer data could be very useful to use MODIS data for the classification of different aerosol types in the absence of Sun photometer data [e.g., *Kahn et al.,* 2005, 2010; *Remer et al.,* 2002, 2005]. A detailed comparison of MODIS AOD with our Sun photometer data is shown in this section. Data provided by MODIS Terra

Table 3. Statistical Parameters of the Comparison Between MODIS/Aqua AOD Versus Sun Photometer AOD[a]

	N	Slope	R^2	MABE (%)	MBE (%)
European/Mediterranean air masses	43	0.88 ± 0.08	0.71	27.6	−27.6
North African air masses	26	1.11 ± 0.13	0.76	13.5	−7.1
Atlantic/Iberian Peninsula air masses	19	0.95 ± 0.07	0.91	33.5	−27.1

[a]MBE, mean bias error; MABE, mean absolute bias error.

and MODIS Aqua over Alborán are compared with Sun photometer data that coincide in time and space. Only those MODIS overpasses included in a square box of 50 × 50 km centered over Alborán (sea surface pixels) were considered for comparison. For the temporal statistical analysis, MODIS overpasses within ±30 min of the Sun photometer measurements were used in the comparison. A scatterplot of the AOD at 550 nm provided by MODIS and the Sun photometer is shown in Figure 8. Ground-based AOD at 550 nm was derived from the Sun photometer data at 500 and 670 nm using the Angström law. The number of simultaneous satellite ground-based data points by platform was 108 for Terra and 107 for Aqua.

Linear regression analysis was performed for both data sets and for each sector. The correlation between MODIS and Sun photometer AOD data was very high, with a coefficient of determination (R^2) between 0.71 and 0.91 depending on the source region considered and the MODIS platform (Figures 8a and 8b). The MABE (mean absolute bias error) parameter also indicated that the agreement was reasonably strong, especially for the North African sector, which is associated with desert dust and higher AOD values (Tables 3 and 4). Moreover, most of the AOD data obtained with the Sun photometer were within the MODIS-estimated uncertainties (±0.03±0.05 (AOD) over ocean) (Figures 8a and 8b). In the case of Terra, the fraction of data within MODIS-estimated uncertainties was approximately 65% for the European/Mediterranean and the Atlantic/Iberian Peninsula sectors and increased to 80% for the North African sector. For Aqua, the fraction of data within MODIS-estimated uncertainties was 70% for the Atlantic/Iberian Peninsula sector and 80% for the North African sector. However, for the European/Mediterranean sector, this value drops to 45%. Considering MODIS-estimated uncertainties, especially for AOD below 0.2, the values provided by the Sun photometer for the European/Mediterranean sector were higher than the values obtained from MODIS.

The slopes of the linear fit between the MODIS and Sun photometer data show that AOD values derived from MODIS underestimate the Sun photometer values during dust conditions (Figures 8a and 8b). The mean bias error (MBE) $((AOD^{MODIS} - AOD^{Sun\ photometer})/AOD^{Sun\ photometer})$ confirms this underestimation, especially in the European/Mediterranean and the Atlantic/Iberian Peninsula sectors (Tables 3 and 4). However, similar studies performed using the ocean algorithm in coastal areas indicated that MODIS overestimates AOD in dust cases and underestimates AOD values during dust-free periods [e.g., *Santese et al.,* 2007; *Bennouna et al.,* 2011]. According to these results, the influence of land when applying the ocean algorithm in coastal areas should be taken into account.

Our results show good agreement between AOD estimated from MODIS using the ocean algorithm and AOD retrieved from Sun photometer measurements and are in accordance with other validation studies [e.g., *Ichoku et al*., 2002; *Levy et al.,* 2005; *Glantz and Tesche*, 2012]. The best agreement is found for cases classified as originating from the North African sector, which presents large aerosol loads usually linked to the transport of desert mineral dust particles. However, further analysis with more data points would improve the representativeness of these results.

Table 4. Statistical Parameters of the Comparison Between MODIS/Terra AOD Versus Sun Photometer AOD[a]

	N	Slope	R^2	MABE (%)	MBE (%)
European/Mediterranean air masses	17	0.75 ± 0.05	0.93	19.7	−18.7
North African air masses	30	0.97 ± 0.11	0.74	14.9	−3.3
Atlantic/Iberian Peninsula air masses	54	0.88 ± 0.08	0.71	32.8	−23.6

[a]MBE, mean bias error; MABE, mean absolute bias error.

5. Conclusions

Eight months of observations (June 2011 to January 2012) of the aerosol optical and microphysical properties were carried out at the remote Alborán Island in the western Mediterranean region. To our knowledge, this is the first study over this region using Sun photometer measurements and inversion products in the almucantar and principal plane configurations. Air masses affecting this area were classified according to three potential aerosol source origins. AOD (440 nm) showed high mean values (0.27 ± 0.12) associated with high mean values of α(440–870 nm) of 1.2 ± 0.3 for air masses transported from the European/Mediterranean sector. For this sector, an increase in AOD(λ) was associated with a shift of α(440–870 nm) toward larger values and more negative $\delta\alpha$ values, indicating an increase in the fine aerosol fraction for larger AODs. The largest aerosol load (mean AOD (440 nm) of 0.38 ± 0.13) associated with the lowest mean value of α(440–870 nm) of 0.6 ± 0.2 was found for air masses originating from the North African sector. The mean α(440–870) value obtained in our study during desert dust intrusions was slightly higher than the reported value for pure dust aerosols near dust source regions and was similar to that obtained for a mixture of dust and fine particles. This result may suggest a mixing of desert dust with fine particles or a reduction in the mean particle size during dust transport to Alborán, due to the deposition of the largest dust particles. In most of the dust intrusions, α was higher than 0.5 and $\delta\alpha \geq 0$, indicating a significant contribution of fine particles to total AOD in these dusty cases. These fine particles were possibly associated with anthropogenic particles originating in urban-industrial areas in North Africa, which were advected with desert dust particles, or to anthropogenic fine particles from ship emissions and/or coming from polluted European regions. The lowest aerosol load conditions during the whole measurement period were found for the North Atlantic Ocean and Iberian Peninsula sector, with mean AOD (440 nm) values of 0.15 ± 0.08 and α(440–870 nm) values of 1.1 ± 0.4. Pure maritime situations associated with AOD < 0.15 and α(440–870) < 1 were found only in the Atlantic/Iberian Peninsula category. We found that only 33% of the data included in the Atlantic/Iberian Peninsula category (40% of all data) were associated with pure maritime situations, indicating the significant influence of aerosols transported from the European and African continents.

The difference between ω(440 nm) obtained for the different aerosol categories associated with the different aerosol source regions was very small. This result represents an advantage for satellite retrievals of AOD at shorter wavelengths of the visible range, because $\omega(\lambda)$ must be assumed a priori in many satellite retrieval algorithms. As expected, $\omega(\lambda)$ increased slightly with wavelength for the North African sector, which is a typical characteristic of desert dust. However, $\omega(\lambda)$ values obtained for the North African sector were lower, especially at the largest wavelengths, than those reported for pure desert dust measured close to dust source regions and were similar to those reported for dust mixed with anthropogenic and/or biomass burning particles. The low $\omega(\lambda)$ values obtained for the North African sector were probably caused by the pickup of fine anthropogenic absorbing particles (i.e., black carbon) during dust transport over North African urban/industrial areas, and/or to the coexistence over Alborán of desert dust and fine absorbing particles emitted from ships or transported from urban-industrial European areas.

A sector classification method applied only to air masses transported from North Africa revealed two main airflow patterns toward Alborán Island, one from northwestern Africa through the Atlantic Ocean (78% of cases) and one from northeastern Africa through the Mediterranean Sea (22% of cases). Whereas air masses from northwestern Africa passed over various urban industrial areas along the coast of Morocco, air masses originating from northeastern Africa reached Alborán Island without traversing many anthropogenic aerosol sources. This analysis revealed that aerosol properties, AOD, α(440–870), and $\omega(\lambda)$ did not show significant differences over Alborán Island during desert dust intrusions coming from these two North African source regions. In addition, a high number of observations during air mass transport from these two North African source regions showed α(440–870) values higher than 0.5 values, indicating aerosol mixtures of different sizes (dust and fine particles) for both sectors. For both North African sectors, the increase of $\omega(\lambda)$ with wavelength was weaker and $\omega(\lambda)$ values were lower, especially at larger wavelengths, than those typically observed for desert dust conditions derived from Sun photometer measurements. Therefore, these results indicate a significant absorbing aerosol contribution during desert dust events arriving from both North African sectors.

One of the important results obtained in this work was the reasonable agreement between AOD estimated from MODIS using the ocean algorithm and AOD retrieved from Sun photometer

measurements. The best agreement was found for cases classified as originating from the North African sector, which were associated with large aerosol loads linked to the transport of desert mineral dust particles. However, further analysis with more data points would improve the representativeness of these results.

Acknowledgments

This work was supported by the Andalusia Regional Government through projects P12-RNM-2409 and P10-RNM-6299, by the Spanish Ministry of Science and Technology through projects CGL2010-18782 and CGL2013-45410-R, by the EU through ACTRIS project (EU INFRA-2010-1.1.16-262254), and by the University of Granada through the contract "Plan Propio. Programa 9. Convocatoria 2013." CIMEL Calibration was performed at the AERONET-EUROPE calibration center (http://aeronet.gsfc.nasa.gov), supported by ACTRIS (European Union Seventh Framework Program (FP7/2007-2013) under grant agreement 262254). Granados-Muñoz was funded under grant AP2009-0552. ALFA database computation was partly supported by RES (Spanish Supercomputation Network) computing resources (projects AECT-2009-1-0012 and AECT-2011-3-0016). The authors express gratitude to the NOAA Air Resources Laboratory (ARL) for the HYSPLIT transport and dispersion model (http://ready.arl.noaa.gov/HYSPLIT.php). We gratefully acknowledge the MODIS mission scientists and associated NASA personnel for the production of the data used in this publication (http://modis.gsfc.nasa.gov/). Finally, the authors gratefully acknowledge the outstanding support received from Royal Institute and Observatory of the Spanish Navy (ROA). We also thank Alexander Smirnov for his help and advice in the preparation of the manuscript.

References

Alados-Arboledas, L., H. Lyamani, and F. J. Olmo (2003), Aerosol size properties at Armilla, Granada (Spain), *Q. J. R. Meteorol. Soc.*, *129*, 1395–1413.

Alados-Arboledas, L., et al. (2008), Aerosol columnar properties retrieved from CIMEL radiometers during VELETA 2002, *Atmos. Environ.*, *42*, 2654–2667.

Basart, S., C. Perez, E. Cuevas, J. M. Baldasano, and G. P. Gobbi (2009), Aerosol characterization in Northern Africa, Northeastern Atlantic, Mediterranean Basin and Middle East from direct-sun AERONET observations, *Atmos. Chem. Phys.*, *9*, 8265–8282.

Bauer, S., E. Bierwirth, M. Esselborn, A. Petzold, A. Macke, T. Trautmann, and M. Wendisch (2011), Airborne spectral radiation measurements to derive solar radiative forcing of Saharan dust mixed with biomass burning smoke particles, *Tellus*, *63B*, 742–750.

Becagli, S., et al. (2012), Evidence for heavy fuel oil combustion aerosols from chemical analyses at the island of Lampedusa: A possible large role of ships emissions in the Mediterranean, *Atmos. Chem. Phys.*, *12*, 3479–3492, doi:10.5194/acp-12-3479-2012.

Bennouna, Y. S., V. E. Cachorro, C. Toledano, A. Berjon, N. Prats, D. Fuertes, R. Gonzalez, R. Rodrigo, B. Torres, and A. M. de Frutos (2011), Comparison of atmospheric aerosol climatologies over Southwestern Spain derived from AERONET and MODIS, *Remote Sens. Environ.*, *115*(5), 1272–1284, doi:10.1016/j.rse.2011.01.011.

Cachorro, V. E., C. Toledano, N. Prats, M. Sorribas, S. Mogo, A. Berjón, B. Torres, R. Rodrigo, J. de la Rosa, and A. M. De Frutos (2008), The strongest desert dust intrusion mixed with smoke over the Iberian Peninsula registered with Sun photometry, *J. Geophys. Res.*, *113*, D14S04, doi:10.1029/2007JD009582.

Chu, D. A., Y. J. Kaufman, L. A. Remer, and B. N. Holben (1998), Remote sensing of smoke from MODIS airborne simulator during the SCAR-B experiment, *J. Geophys. Res.*, *103*, 31,979–31,987.

Chu, D. A., Y. J. Kaufman, C. Ichoku, L. A. Remer, D. Tanre, and B. N. Holben (2002), Validation of MODIS aerosol optical depth retrieval over land, *Geophys. Res. Lett.*, *29*, doi:10.1029/2001GL013205.

Cofala, J., M. Amann, Z. Klimont, K. Kupiainen, and L. Höoglund-Isaksson (2007), Scenarios of global anthropogenic emissions of air pollutants and methane until 2030, *Atmos. Environ.*, *38*, 4769–4778, doi:10.1016/j.atmosenv.2007.07.010.

Derimian, Y., A. Karnieli, Y. J. Kaufman, M. O. Andreae, T. W. Andreae, O. Dubovik, W. Maenhaut, and I. Koren (2008), The role of iron and black carbon in aerosol light absorption, *Atmos. Chem. Phys.*, *8*, 3623–3637.

Di Biagio, C., A. di Sarra, D. Meloni, F. Monteleone, S. Piacentino, and D. Sferlazzo (2009), Measurements of Mediterranean aerosol radiative forcing and influence of the single scattering albedo, *J. Geophys. Res.*, *114*, D06211, doi:10.1029/2008JD011037.

di Sarra, A., T. Di Iorio, M. Cacciani, G. Fiocco, and D. Fuà (2001), Saharan dust profiles measured by lidar at Lampedusa, *J. Geophys. Res.*, *106*, 10,335–10,347.

Draxler, R. R., and G. Rolph (2003), HYSPLIT (Hybrid Single-Particle Lagrangian Integrated Trajectory) model, NOAA Air Resour. Lab., Silver Spring, Md. [Available at http://www.arl.noaa.gov/ready/hysplit4.html.]

Dubovik, O., B. Holben, T. F. Eck, A. Smirnov, Y. J. Kaufman, M. D. King, D. Tanre, and I. Slutsker (2002), Variability of absorption and optical properties of key aerosol types observed in worldwide locations, *J. Atmos. Sci.*, *59*, 590–608.

Eck, T. F., B. N. Holben, J. S. Reid, O. Dubovik, A. Smirnov, N. T. O'Neill, I. Slutsker, and S. Kinne (1999), Wavelength dependence of optical depth of biomass burning, urban, and desert dust aerosols, *J. Geophys. Res.*, *104*, 31,333–31,349.

Eck, T. F., et al. (2010), Climatological aspects of the optical properties of fine/coarse mode aerosol mixtures, *J. Geophys. Res.*, *115*, D19205, doi:10.1029/2010JD014002.

Estellés, V., J. A. Martinez-Lozano, and M. A. P. Utrillas (2007), Influence of air mass history on the columnar aerosol properties at Valencia, Spain, *J. Geophys. Res.*, *112*, D15211, doi:10.1029/2007JD008593.

Gerasopoulos, E., M. O. Andreae, C. S. Zerefos, T. W. Andreae, D. Balis, P. Formenti, P. Merlet, V. Amiridis, and C. Papastefanou (2003), Climatological aspects of aerosol optical properties in Northern Greece, *Atmos. Chem. Phys.*, *3*, 2025–2041.

Gerasopoulos, E., G. Kouvarakis, P. Babasakalis, M. Vrekoussis, J. P. Putaud, and N. Mihalopoulos (2006), Origin and variability of particulate matter (PM10) mass concentrations over the Eastern Mediterranean, *Atmos. Environ.*, *40*, 4679–4690.

Gerasopoulos, E., P. Kokkalis, V. Amiridis, E. Liakakou, C. Perez, K. Haustein, K. Eleftheratos, M. O. Andreae, T. W. Andreae, and C. S. Zerefos (2009), Dust specific extinction cross-sections over the Eastern Mediterranean using the BSC-DREAM model and sun photometer data: The case of urban environments, *Ann. Geophys.*, *27*, 2903–2912.

Gerasopoulos, E., V. Amiridis, S. Kazadzis, P. Kokkalis, K. Eleftheratos, M. O. Andreae, T. W. Andreae, H. El-Askary, and C. S. Zerefos (2011), Three-year ground based measurements of aerosol optical depth over the Eastern Mediterranean: The urban environment of Athens, *Atmos. Chem. Phys.*, *11*, 2145–2159.

Glantz, P., and M. Tesche (2012), Assessment of two aerosol optical thickness retrieval algorithms applied to MODIS Aqua and Terra measurements in Europe, *Atmos. Meas. Tech.*, *5*, 1727–1740, doi:10.5194/amt-5-1727-2012.

Gobbi, G. P., Y. J. Kaufman, I. Koren, and T. F. Eck (2007), Classification of aerosol properties derived from AERONET direct sun data, *Atmos. Chem. Phys.*, *7*, 453–458.

Hand, V., G. Capes, D. Vaughan, P. Formenti, J. M. Haywood, and H. Coe (2010), Evidence of internal mixing of African dust and biomass burning particles by individual particle analysis using electron beam techniques, *J. Geophys. Res.*, *115*, D13301, doi:10.1029/2009JD012938.

Holben, B. N., et al. (1998), AERONET—A federated instrument network and data archive for aerosol characterization, *Remote Sens. Environ.*, *66*, 1–16.

Ichoku, C., D. A. Chu, S. Mattoo, Y. J. Kaufman, L. A. Remer, D. Tanré, I. Slutsker, and B. N. Holben (2002), A spatio-temporal approach for global validation and analysis of MODIS aerosol products, *Geophys. Res. Lett.*, *29*(12), 8006, doi:10.1029/2001GL013206.

Ichoku, C., Y. J. Kaufman, L. A. Remer, and R. Levy (2004), Global aerosol remote sensing from MODIS, *Adv. Space Res.*, *34*, 820–827.

Intergovernmental Panel on Climate Change (2013), *Climate Change 2013: The Physical Science Basis. Contribution of Working Group I to the Fifth Assessment Report of the Intergovernmental Panel on Climate Change*, edited by T. F. Stocker et al., 1535 pp., Cambridge Univ. Press, Cambridge, U. K., and New York.

Kahn, R. A., B. J. Gaitley, J. V. Martonchik, D. J. Diner, K. A. Crean, and B. Holben (2005), Multiangle Imaging Spectroradiometer (MISR) global aerosol optical depth validation based on 2 years of coincident Aerosol Robotic Network (AERONET) observations, *J. Geophys. Res.*, *110*, D10S04, doi:10.1029/2004JD004706.

Kahn, R. A., B. J. Gaitley, M. J. Garay, D. J. Diner, T. F. Eck, A. Smirnov, and B. N. Holben (2010), Multiangle Imaging SpectroRadiometer global aerosol product assessment by comparison with the Aerosol Robotic Network, *J. Geophys. Res.*, *11*, D23209, doi:10.1029/2010JD014601.

Kaskaoutis, D. G., S. K. Kharol, P. R. Sinha, R. P. Singh, H. D. Kambezidis, A. R. Sharma, and K. V. S. Badarinath (2011), Extremely large anthropogenic-aerosol contribution to total aerosol load over the Bay of Bengal during winter season, *Atmos. Chem. Phys.*, *11*, 7097–7117.

Kaufman, Y. J. (1993), Aerosol optical thickness and atmospheric path radiance, *J. Geophys. Res.*, *98*, 2677–2692.

Kaufman, Y. J., D. Tanré, H. R. Gordon, T. Nakajima, J. Lenoble, R. Frouin, H. Grassl, B. M. Herman, M. D. King, and P. M. Telllet (1997), Passive remote sensing of tropospheric aerosol and atmospheric correction for the aerosol effect, *J. Geophys. Res.*, *102*(D14), 16,815–16,830, doi:10.1029/97JD01496.

Kaufman, Y. J., et al. (1998), Smoke, Clouds and Radiation-Brazil (SCAR-B) experiment, *J. Geophys. Res.*, *103*, 31,783–31,808.

King, M., Y. Kaufman, D. Tanré, and T. Nakajima (1999), Remote sensing of tropospheric aerosols from space: Past, present, and future, *Bull. Am. Meteorol. Soc.*, *80*(11), 2229–2259.

Levy, R. C., L. A. Remer, J. V. Martins, Y. J. Kaufman, A. Plana-Fattori, J. Redemann, and B. Wenny (2005), Evaluation of the MODIS aerosol retrievals over ocean and land during CLAMS, *J. Atmos. Sci.*, *62*, 974–992.

Lyamani, H., F. J. Olmo, A. Alcantara, and L. Alados-Arboledas (2006a), Atmospheric aerosols during the 2003 heat wave in southeastern Spain I: Spectral optical depth, *Atmos. Environ.*, *40*, 6453–6464.

Lyamani, H., F. J. Olmo, A. Alcántara, and L. Alados-Arboledas (2006b), Atmospheric aerosols during the 2003 heat wave in southeastern Spain II: Microphysical columnar properties and radiative forcing, *Atmos. Environ.*, *40*, 6465–6476.

Lyamani, H., A. Valenzuela, D. Perez-Ramirez, A. Smirnov, C. Toledano, M. J. Granados-Muñoz, F. J. Olmo, and L. Alados-Arboledas (2014), Aerosol properties over western Mediterranean basin: Temporal and spatial variability, *Atmos. Chem. Phys. Discuss.*, *14*, 21,523–21,564.

Meloni, D., A. di Sarra, G. Pace, and F. Monteleone (2006), Aerosol optical properties at Lampedusa (Central Mediterranean): 2. Determination of single scattering albedo at two wavelengths for different aerosol types, *Atmos. Chem. Phys.*, *6*, 715–727.

Meloni, D., A. di Sarra, G. Biavati, J. J. DeLuisi, F. Monteleone, G. Pace, S. Piacentino, and D. Sferlazzo (2007), Seasonal behavior of Saharan dust events at the Mediterranean island of Lampedusa in the period 1999–2005, *Atmos. Environ.*, *41*, 3041–3056.

Meloni, D., A. di Sarra, F. Monteleone, G. Pace, S. Piacentino, and D. M. Sferlazzo (2008), Seasonal transport patterns of intense Saharan dust events at the Mediterranean island of Lampedusa, *Atmos. Res.*, *88*, 134–148.

Millán, M., R. Salvador, and E. Mantilla (1996), Meteorology and photochemical air pollution in southern Europe: Experimental results from EC research projects, *Atmos. Environ.*, *30*(12), 1909–1924.

Nakajima, T., G. Tonna, R. Z. Rao, P. Boi, Y. Kaufman, and B. Holben (1996), Use of sky brightness measurements from ground for remote sensing of particulate polydispersions, *Appl. Opt.*, *35*, 2672–2686.

Olmo, F. J., A. Quirantes, A. Alcantara, H. Lyamani, and L. Alados-Arboledas (2006), Preliminary results of a non-spherical aerosol method for the retrieval of the atmospheric aerosol optical properties, *J. Quant. Spectrosc. Radiat. Transfer*, *100*, 305–314.

Olmo, F. J., A. Quirantes, V. Lara, H. Lyamani, and L. Alados-Arboledas (2008), Aerosol optical properties assessed by an inversion method using the solar principal plane for non-spherical particles, *J. Quant. Spectrosc. Radiat. Transfer*, *109*, 1504–1516.

Pace, G., A. di Sarra, D. Meloni, S. Piacentino, and P. Chamard (2006), Aerosol optical properties at Lampedusa (Central Mediterranean). 1. Influence of transport and identification of different aerosol types, *Atmos. Chem. Phys.*, *6*, 697–713.

Pandolfi, M., Y. Gonzalez-Castanedo, A. Alastuey, J. D. de la Rosa, E. Mantilla, A. Sánchez de la Campa, X. Querol, J. Pey, F. Amato, and T. Moreno (2011), Source apportionment of PM10 and PM2.5 at multiple sites in the strait of Gibraltar by PMF: Impact of shipping emissions, *Environ Sci Pollut Res.*, *18*, 260–269, doi:10.1007/s11356-010-0373-4.

Pereira, S. N., F. Wagner, and A. M. Silva (2011), Seven years of measurements of aerosol scattering properties, near the surface, in the southwestern Iberia Peninsula, *Atmos. Chem. Phys.*, *11*, 17–29.

Perrone, M. R., and A. Bergamo (2011), Direct radiative forcing during Sahara dust intrusions at a site in the Central Mediterranean: Anthropogenic particle contribution, *Atmos. Res.*, *101*, 783–798.

Petzold, A., et al. (2008), Saharan dust absorption and refractive index from aircraft-based observations during SAMUM 2006, *Tellus*, *61B*, doi:10.1111/j.1600-0889.2008.00383.x.

Prats, N., V. E. Cachorro, M. Sorribas, S. Mogo, A. Berjon, C. Toledano, A. M. De Frutos, J. de la Rosa, N. Laulainen, and B. A. de la Morena (2008), Columnar aerosol optical properties during "El Arenosillo 2004 summer campaign", *Atmos. Environ.*, *42*, 2643–2653.

Remer, L. A., Y. J. Kaufman, Z. Levin, and S. Ghan (2002), Model assessment of the ability of MODIS to measure top-of-atmosphere direct radiative forcing from smoke aerosols, *J. Atmos. Sci.*, *59*, 657–667.

Remer, L. A., et al. (2005), The MODIS aerosol algorithm, products and validation, *J. Atmos. Sci.*, *62*, 947–973, doi:10.1175/JAS3385.1.

Rodríguez, S., A. Alastuey, S. Alonso-Perez, X. Querol, E. Cuevas, J. Abreu-Afonso, M. Viana, N. Pérez, M. Pandolfi, and J. de la Rosa (2011), Transport of desert dust mixed with North African industrial pollutants in the subtropical Saharan Air Layer, *Atmos. Chem. Phys.*, *11*, 6663–6685.

Romero, R., G. Sumner, C. Ramis, and A. Genovés (1999), A classification of the atmospheric circulation patterns producing significant daily rainfall in the Spanish Mediterranean area, *Int. J. Climatol.*, *19*, 765–785.

Rozwadowska, A., T. Zielinski, T. Petelski, and P. Sobolewski (2010), Cluster analysis of the impact of air back-trajectories on aerosol optical properties at Hornsund, Spitsbergen, *Atmos. Chem. Phys.*, *10*, 877–893.

Santese, M., F. De Tomasi, and M. R. Perrone (2007), Moderate resolution imaging spectroradiometer (MODIS) and aerosol robotic network (AERONET) retrievals during dust outbreaks over the Mediterranean, *J. Geophys. Res.*, *112*, D18201, doi:10.1029/2007JD008482.

Silva, A. M., M. L. Bugalho, M. J. Costa, W. Von Hoyningen-Huene, T. Schmidt, J. Heintzenberg, and S. Henning (2002), Aerosol optical properties from columnar data during the second Aerosol Characterization Experiment on the south coast of Portugal, *J. Geophys. Res.*, *107*(D22), 4642, doi:10.1029/2002JD002196.

Smirnov, A., O. Yershov, and Y. Villevalde (1995), Measurement of aerosol optical depth in the Atlantic Ocean and the Mediterranean Sea, *SPIE*, *2582*, 203–214.

Smirnov, A., B. N. Holben, T. F. Eck, O. Dubovik, and I. Slutsker (2000), Cloud-screening and quality control algorithms for the AERONET database, *Remote Sens Rev.*, *73*, 337–349.

Smirnov, A., B. N. Holben, Y. J. Kaufman, O. Dubovik, T. F. Eck, I. Slutsker, C. Pietras, and R. N. Halthore (2002), Optical properties of atmospheric aerosol in maritime environments, *J. Atmos. Sci.*, *59*, 501–523.

Smirnov, A., et al. (2009), Maritime Aerosol Network as a component of Aerosol Robotic Network, *J. Geophys. Res.*, *114*, D06204, doi:10.1029/2008JD011257.

Stohl, A. (1998), Computation, accuracy and applications of trajectories: A review and bibliography, *Atmos. Environ.*, *32*, 947–966.
Sumner, G., V. Homar, and C. Ramis (2001), Precipitation seasonality in eastern and southern coastal Spain, *Int. J. Climatol.*, *21*, 219–247.
Tafuro, A. M., F. Barnaba, F. De Tomasi, M. R. Perrone, and G. P. Gobbi (2006), Saharan dust particle properties over the central Mediterranean, *Atmos. Res.*, *81*, 67–93.
Tanré, D., Y. Kaufman, M. Herman, and S. Mattoo (1997), Remote sensing of aerosol properties over oceans using the MODIS/EOS spectral radiances, *J. Geophys. Res.*, *102*(D14), 16,971–16,988.
Tesche, M., et al. (2009), Vertical profiling of Saharan dust with Raman lidars and airborne HSRL in southern Morocco during SAMUM, *Tellus*, *61B*, 144–164.
Toledano, C., V. E. Cachorro, A. M. de Frutos, M. Sorribas, N. Prats, and B. A. de la Morena (2007), Inventory of African desert dust events over the southwestern Iberian Peninsula in 2000–2005 with an AERONET Cimel Sun photometer, *J. Geophys. Res.*, *112*, D21201, doi:10.1029/2006JD008307.
Toledano, C., V. E. Cachorro, A. M. de Frutos, B. Torres, A. Berjon, M. Sorribas, and R. S. Stone (2009), Airmass classification and analysis of aerosol types at El Arenosillo (Spain), *J. Appl. Meteorol. Climatol.*, *48*, 962–981.
Toledano, C., et al. (2011), Optical properties of aerosol mixtures derived from sun-sky radiometry during SAMUM-2, *Tellus*, *63B*, 635–648.
Valenzuela, A., F. J. Olmo, H. Lyamani, M. Antón, A. Quirantes, and L. Alados-Arboledas (2012a), Analysis of the desert dust radiative properties over Granada using principal plane sky radiances and spheroids retrieval procedure, *Atmos. Res.*, doi:10.1016/j.atmosres.2011.11.005.
Valenzuela, A., F. J. Olmo, H. Lyamani, M. Antón, A. Quirantes, and L. Alados-Arboledas (2012b), Classification of aerosol radiative properties during African desert dust intrusions over southeastern Spain by sector origins and cluster analysis, *J. Geophys. Res.*, *117*, D06214, doi:10.1029/2011JD016885.
Valenzuela, A., F. J. Olmo, H. Lyamani, M. Antón, A. Quirantes, and L. Alados-Arboledas (2012c), Aerosol radiative forcing during African desert dust intrusions (2005–2010) over Southeastern Spain, *Atmos. Chem. Phys.*, *12*, 10,331–10,351.
Valenzuela, A., F. J. Olmo, M. Antón, H. Lyamani, G. Titos, A. Cazorla, and L. Alados-Arboledas (2014), Aerosol scattering and absorption Angström exponent as indicators of dust and dust-free days over Granada (Spain), *Atmos. Res.*, *D-14-00217*, doi:10.1016/j.atmosres.2014.10.015.
Viana, M., F. Amato, A. Alastuey, X. Querol, T. Moreno, S. G. Dos Santos, M. D. Herce, and R. Fernández-Patier (2009), Chemical tracers of particulate emissions from commercial shipping, *Environ. Sci. Technol.*, *43*(19), 7472–7477.
Wagner, F., and A. M. Silva (2008), Some considerations about Angstrom exponent distributions, *Atmos. Chem. Phys.*, *8*(3), 481–489.
Xia, X., H. Chen, and W. Zhang (2007), Analysis of the dependence of column-integrated aerosol properties on long-range transport of air masses in Beijing, *Atmos. Environ.*, *41*, 7739–7750.